Simultaneous Increase in CO_2 Permeability and Selectivity by BIT-72 and Modified BIT-72 based Mixed Matrix Membranes

Nain Tara[1], Zufishan Shamair[1,2], Nitasha Habib[1], Michael Craven[3], Muhammad Roil Bilad[4], Muhammad Usman[5], Xin Tu[3**], Asim Laeeq Khan[1*]

[1] Department of Chemical Engineering, COMSATS University Islamabad, Lahore Campus, Pakistan

[2] School of Computing, Engineering and Digital Technologies, Teesside University, Middlesbrough, TS1 3BX, United Kingdom

[3] Department of Electrical Engineering and Electronics, University of Liverpool, Liverpool L69 3GJ, United Kingdom

[4] Faculty of Integrated Technologies, Universiti Brunei Darussalam, Gadong BE1410, Brunei

[5] Center of Research Excellence in Nanotechnology, King Fahd University of Petroleum and Minerals (KFUPM), Dharan 31261, Saudi Arabia

* alaeeqkhan@cuilahore.edu.pk

** Xin.Tu@liverpool.ac.uk

Abstract

Gas separation membranes are a key development in eradication of harmful greenhouse gases such as carbon dioxide (CO_2). Different strategies have been utilized to enhance membrane performance and to overcome their drawbacks. In this study a unique approach has been utilized to enhance membrane performance. Initially mixed matrix membranes (MMM) were fabricated with a novel metal organic framework (MOFs), namely BIT-72 incorporated in Pebax®1657 matrix. At 30% loading of BIT-72, CO_2/CH_4 and CO_2/N_2 selectivities of 30.96 and 56.28 were achieved respectively with CO_2 permeability of 139 Barrer. To further enhance the performance of the MMM, BIT-72 was treated with plasma of N_2 or O_2 gases to prepare MMMs with same polymer (N_2-BIT-72 MMM and O_2-BIT-72 MMM, respectively). As a result, CO_2/CH_4 and CO_2/N_2 selectivity was enhanced to 43.07 and 72.64 respectively for N_2 treated BIT-72 MMM (CO_2 permeability 146 Barrer) and for O_2 treated BIT-72 MMM (CO_2 permeability 145 Barrer)

CO_2/CH_4 and CO_2/N_2 selectivity was increased to 37.28 and 66.21 respectively. Plasma modified BIT-72 MMM showcased promising results for further applications.

Keywords: CO_2 capture; Metal-Organic Framework; Mixed Matrix Membranes; BIT-72, Plasma Treatment

1. Introduction

Global industrialization and accelerated demand of energy produced from fossil fuels are leading to enormous emissions of carbon dioxide (CO_2) [1]. CO_2 constitutes about 80% of greenhouse gases (GHGs) which is the prime reason of global warming and its adverse aftermaths [2]. This pervasive situation must be overcome by developing energy efficient CO_2 capture technologies [3]. Conventional techniques, including dual-alkali absorption, molecular sieve adsorbents, cryogenic separation and amine scrubbing, are efficient but all of these processes are extremely energy intensive [4, 5]. For instance, amine scrubbing consumes 4-6 GJ/ton of CO_2 recovered solely for its solvent regeneration step [6]. Post-combustion CO_2 separation is one of the most convenient mechanisms for all industrial plants as it is easy to retrofit to pre-existing systems, and this separation process has been subjected to many developments over the years [7, 8].

Membrane technology is a promising alternative to energy intensive conventional technologies. Polymeric membranes provide the advantageous traits for various applications particularly gas separation [9-11]. The use of modified membranes is highly desirable on account of their striking traits such as modularity, easy integration, environmentally friendly process and most significantly low costs [12, 13]. The potential advantages associated with membranes make them attractive for post-combustion CO_2 capture and sweetening of natural gas. However, membrane-based processes face certain limitations such as high moisture content, robust temperature-pressure conditions, corrosive impurities and extremely low concentration of CO_2 i.e., 10-15% [14]. Different routes have been tried to overcome these problems but still fall short [15, 16]. To enhance membrane performance and overcome these problems, a distinct form of membranes called mixed matrix membranes (MMMs) are prepared by impregnating polymer membranes with certain inorganic particles i.e., carbon molecular sieves, zeolites, etc. [8, 17]. These multifunctional MMMs combine higher selectivity and robust stabilities of the inorganic particles with the intrinsically permeable

and mechanical strength of the polymer. These MMMs are, therefore, more resilient, processable and economical [18].

A rapidly emerging technology in the preparation of MMMs is the use of metal-organic frameworks (MOFs) that are basically organic-inorganic hybrids. MOFs are composed of complex assembly of subunits that can be arranged in multiple configurations depending upon the functionality of the organic ligands and how they are linked to central metal-based nodes [19, 20]. The unique structural attributes of MOFs make them engineer-able materials and endow them with controllable porosity, optimized pore dimensions, tunable chemical functionality, incredibly higher surface areas, systematic framework and adjustable affinity towards distinct gases. Different approaches can be adopted to customize the structures of MOFs providing wide margins for innovation that has provoked scientists to penetrate deep into this field and find economical and efficient solutions for atmospheric pollution.

Numerous research groups have conducted studies that incorporate different MOFs and polymers to prepare MMMs for CO_2 capture. MOFs alone are responsible for enhancing gas separation performance by these materials. Deng et al. used ZIF-C to prepare MMMs with Pebax®1657 and reported that these MOFs enhanced permeability [21]. Habib et al. used NOTT-300 and Pebax®1657 for the preparation of MMMs used to separate CO_2 from CH_4 and N_2 [22]. The authors reported a simultaneous increase in permeability and selectivity with increasing MOF loading for both CH_4 and N_2 gas mixtures. Enhancing MOF properties by physical and chemical means is also an interesting approach. Yasmeen et al. combined ZIF-67 and polysulfone and compared its ability to capture CO_2 with that of ionic liquid modified ZIF-67 [23]. They achieved better results for the ionic liquid modified ZIF67 membranes compared to the pure ZIF-67/polysulfone membranes. Chuah et al. modified UiO-66 by chemically functionalizing it with NH_2 groups and used polyimide to make MMMs [24].

Modification of a MOF surface through plasma treatment is an efficient, green, upgradeable and quickly applied method [25]. Plasma is defined as an ionized gas at quasi-neutral state, wherein electron density is balanced by the concentration of positive ions [26]. It is a multicomponent system that contains free radicals, electrons, photons, energetic ions, excited states and neutral atoms or molecules which collectively make plasma electrically conductive and extremely reactive [26]. In plasma treatment, ionized gases i.e. O_2, N_2, NH_3, Ar, He, H_2 are used to modify the surface

properties of the substrate through oxidation, reduction, crosslinking or ablation reactions which either functionalize the surface, remove contaminants or customize the substrate porosity [27, 28]. For example, Dectose et al. used perfluorohexane plasma to improve the stability of HKUST-1, while Park et al. reported improved acid-base surface energetics of carbon black after N_2 plasma treatment [29, 30].

Aluminum-based and hydroxyl-functionalized MOF with the chemical formula $[Al_4(OH)_2(OCH_3)_4(OH\text{-}BDC)_3]\cdot xH2O$ was recently designed by Li et al. [31]. This innovative MOF, called BIT-72, is tailored to be applied exclusively in post-combustion applications with balanced CO_2 and H_2O selectivities. The BIT-72 crystals are comprised of two types of cages, distorted octahedral and distorted tetrahedral, with corresponding larger and smaller pore sizes [31]. Most MOFs are liable to collapse in the presence of moisture [32] but BIT-72 exhibits high stability, even in acidic and humid conditions, which can be ascribed to high valent Al^{+3}. It has high surface areas, permanent porosity, robust thermal and chemical stability and great CO_2 affinity, thus it is a pertinent choice for post-combustion CO_2 separation and natural gas sweetening [31].

Pebax®1657 is a high-performance polymer comprising 60% of rubbery PEO phase and 40% glassy PA phase and hence is expected to be more compatible with organic ligands of MOF [33]. Pebax®1657 copolymer has been reported to have sublime characteristics such as high durability and flexibility [34], excessive mechanical and thermal stability [35], favorable selectivity for nonpolar gases like N_2 and CH_4 and higher attractions for polar CO_2 [36].

In this work, we incorporated BIT-72 in Pebax®1657 polymer matrix to fabricate MMMs with different MOF loading and evaluated the performances for CO_2 capture. The aim of this study is to introduce a new class of MMMs by combining the extraordinary attributes of both the BIT-72 and Pebax®1657, expecting a promising contribution to post combustion CO_2 separation and natural gas sweetening. The role of BIT-72 has been thoroughly investigated in this study with gas separation of pure and mixed gas. In an effort to further enhance BIT-72 properties for CO_2 capture we further treated the surface of BIT-72 with O_2 and N_2 plasma and tested the plasma-modified BIT-72 embedded MMMs for separation of CO_2.

2. Experimental

2.1. Materials

Aluminum chloride hexahydrate ($AlCl_3 \cdot 6H_2O$) was purchased from Carlo Erba Reagents (France), organic linker 2-hydrox-1,4-benzendicarboxylicacid was purchased from Tokyo Chemical Industry Co. LTD (Japan), and methanol was obtained from Fisher Scientific Limited (U.K). N,N, dimethylformamide (DMF) and ethanol were supplied by Sigma-Aldrich Co. (USA) and Merck KGaA (Germany) respectively. For membrane fabrication, Pebax®1657 was kindly provided by Arkema (France).

2.2. Synthesis of BIT-72

BIT-72 was synthesized by following the procedure reported by Li and coworkers [31]. $AlCl_3 \cdot 6H_2O$ (3.94g, 16.34 mmol) and 2-hydrox-1,4-benzendicarboxylic acid (1.0g, 5.49 mmol) were dissolved in 60 ml of methanol. The resultant mixture was transferred to Teflon lined autoclave and heated at 125 °C for 5 h. The reaction mixture was then cooled to room temperature and white colored crystals were separated through centrifugation at 7000 rpm for 10 min. The product was washed three times with various solvents i.e., deionized water, DMF and methanol, to remove impurities and unreacted species. Finally, the collected product was dried in oven at 70 °C overnight.

2.3. Plasma modification of BIT-72

A coaxial dielectric barrier discharge (DBD) reactor comprised of a quartz tube (300 mm length, 25 mm outer diameter and 2.5 mm thickness), an aluminum foil ground electrode (50 mm length = length of discharge zone) and a stainless steel rod high voltage electrode (17 mm diameter) was used for plasma treatment of BIT-72. Firstly, the crystals of BIT-72 were pelletized, crushed and sieved to 60-40 mesh particle size. 0.15 g of the sieved BIT-72 was then partially packed into the discharge area of the DBD reactor and was held in place using quartz wool plugs positioned at either end of the discharge zone. The plasma was generated using either O_2 or N_2 at a discharge power of 6 W and a gas flow rate of 50 ml/min. The applied voltage and current were measured using a TESTEC HVP-1HF high voltage probe and Bergoz CT-E0.5 current monitor, respectively. The amount of charge accumulated in the DBD was determined by measuring the voltage on the external capacitor (0.47 μF). All electrical signals were monitored and sampled using a Tektronix

MDO 3024 four-channel digital oscilloscope. The discharge power was calculated using the Q-U Lissajous method and controlled using a real-time power monitoring system [37]. The sample was treated with the plasma for 20 min and then allowed to cool for 5 min under the continued flow of the gas. Afterwards, the plasma-treated sample was quickly transferred to a dried vial that was then sealed with a septum cap. The vial was then flushed with Ar for 5 min to store the plasma-treated BIT-72 under an inert atmosphere. After treatment with N_2-plasma, the white color of BIT-72 was retained, however, the O_2-plasma-treated BIT-72 turned yellow.

2.4. Fabrication of MMMs

Solution casting followed by evaporation techniques were used for the synthesis of all the membranes. Before fabrication, polymer pellets and BIT-72 were dried at 80 °C overnight to remove any moisture content. The pristine membrane was prepared by dissolving 5 wt% Pebax®1657 in ethanol/DI water solvent (mass ratio 70:30) through continuous stirring under reflux at 90 °C for 4 h. The polymer solution was then casted on a Teflon petri dish and covered with an inverted funnel for controlled evaporation at ambient conditions for 48 h. Afterwards, it was dried at 60 °C for 12 h to remove any residual solvent. The resultant membrane was transparent and without any visible defects.

MMMs with different BIT-72 loadings (10%, 20%, 30%) were prepared by dispersing corresponding amount of BIT-72 in ethanol/water solvent under reflux at 90 °C for 2 h. The solution was then sonicated for 30 min to avoid agglomeration of BIT-72 particles. Afterwards, half of the calculated amount of Pebax®1657 was added and allowed to dissolve under reflux for 4 h. The remaining polymer was then added before sonication of the resultant mixture for another 30 min to ensure fine dispersion of BIT-72 in the polymer. After 24 h of mixing under reflux and subsequent sonication, the resultant solution was immediately poured onto a Teflon petri dish and allowed to dry in the same way as of the pristine membrane. The prepared membranes were carefully peeled off and stored in a desiccator. Pebax®1657/30% O_2-BIT-72 and Pebax®1657/30% N_2-BIT-72 were fabricated following the same procedure using O_2-plasma modified BIT-72 (O_2-BIT-72) and N_2-plasma modified BIT-72 (N_2-BIT-72).

2.5. *Characterization techniques*

The crystallinity of BIT-72 and MMMs were studied by X-ray diffraction (XRD) (PANalytical X'Pert Powder DY-3805 that used CuKα (λ=1.54 Å) radiation (2θ) in range between 5° and 50°. The functional group identification was done by fourier transform infrared (FTIR) spectroscopy using Thermo-Nicolet 6700P Spectrometer. Scanning electron microscopy (SEM) for morphological analysis of BIT-72 was performed by TESCAN Vega3 LMU. The SEM of the cross-sectional area of membranes was obtained on FE-SEM: JEOS JSM 6700F. The densities of MMMs were determined via gas pycnometer (G-DenPyc 2900, Gold App Instruments). The fractional free volume (FFV) of the pure Pebax®1657 membrane was calculated using the group contribution method (GCM) as shown in Eq. 1:

$$FFV = \frac{V - 1.3V_w}{V} \quad (1)$$

where, V (cm^3) is the experimentally calculated specific volume of Pebax®1657, and V_w is the van der Waals volume determined by GCM. The FFV of the Pebax®1657/BIT-72 membranes were obtained from the Eq. 2:

$$FFV = \frac{V - \left[\left(\frac{1.3V_w}{M}\right)(1 - \varphi_{BIT72}) + \left(\frac{\varphi_{BIT72}}{\rho_{BIT72}}\right)\right]}{V} \quad (2)$$

where, V (cm^3) is the specific volume of the Pebax®1657/BIT-72 membranes determined experimentally, M (g/mol) is the molecular weight of Pebax®1657 and φ_{BIT72} is the volume fraction of the MOF in the membranes. The volume fraction of the MOF is calculated using Eq. 3:

$$\varphi = \frac{(\omega_{BIT72}/\rho_{BIT72})}{(1 - \omega_{BIT72}/\rho_{BIT72}) + (\omega_{BIT72}/\rho_{BIT72})} \quad (3)$$

where ω_{BIT72} is the weight fraction of BIT-72 in the membranes, ρ_{Pebax} and ρ_{BIT72} (g/cm^3) are the densities of Pebax®1657 and BIT-72 respectively. The theoretical densities are calculated by Eq. 4:

$$\rho_t = \frac{1}{(1 - \omega_{BIT72}/\rho_{BIT72}) + (\omega_{BIT72}/\rho_{BIT72})} \quad (4)$$

The temperature dependency of CO_2 on permeability can be determined through the use of the Arrhenius Equation [38]:

$$P = P_o exp \frac{-E_P}{RT} \quad (5)$$

where P is permeability, P_o is pre-exponential factor, E_p is activation energy, R is the universal gas constant and T represents temperature.

2.6. Gas Permeation Measurements

Membrane performances were tested for both pure gas and mixed gas (CO_2, CH_4, and N_2) feed streams using a custom-built setup under isochoric conditions. The schematic diagram of the permeation cell is illustrated in Figure 1, while the detailed procedure and mechanism have been explained in an earlier study [39]. Before starting the analysis, the cell was kept under vacuum for 8 h to remove any trapped gas or air. Membranes were mounted on porous metallic plates and tightly packed with Viton O-rings. The flow rate and feed composition were controlled by mass flow controllers while the upstream pressure was maintained with a back pressure regulator on the purge line. The maximum upstream pressure and feed flow rate were set as 10 bar and 1 L/min respectively. The constant feed composition was ensured by purging a fraction of the feed flow as retentate. The membrane module was equipped with a heating system that adjusted the temperature from 298 K-338 K accordingly. The permeate lines left the membrane and passed through compact gas chromatograph (CGC, YL Instruments, South Korea) for composition analysis. The flux was determined by connecting the permeate lines to auxiliary cylinder by changing the position of relevant valve. The pressure inside the auxiliary cylinder was allowed to rise until it reached the maximum limit. The rate of increase of pressure (dP/dt) was measured. The gas permeability P_i (where i could be CO_2, CH_4 and N_2) was calculated when permeation reached a steady-state using Eq. 6 [40]:

$$P_i = \frac{273 \times 10^6}{760} \times \frac{y_i V}{AT(76/14.7)x_i P_2} \times \frac{dP}{dt} \quad (6)$$

where P_i is gas permeability in Barrer, x_i and y_i are the upstream and downstream mole fractions of component 'i', respectively, V is the downstream volume (cm^3), T is the operating temperature (K), A refers to the membrane permeation area (cm^2), and P_2 is the feed gas pressure (bar). The transport properties were measured using the time-lag method. A constant volume (50 cm^3) auxiliary cylinder equipped with a pressure transducer was connected to a vacuum pump at one side that kept the pressure negligible, while test gas was introduced from the other side until steady-

state conditions were achieved. The rise in the rate of pressure to the maximum limit was plotted and the intercept was used to determine the time lag, θ, that is related to diffusion coefficient D_i and membrane thickness as Eq. 7 [41]:

$$D_i = \frac{l^2}{6\theta} \quad (7)$$

After calculation of D_i and P_i from respective equations, the solubility coefficient, $S_{i,}$ is calculated using Eq. 8 using. The transport of gases through these membranes follows the solution-diffusion mechanism, represented by the Eq. (8):

$$P_i = S_i \times D_i \quad (8)$$

The mixed gas selectivity α_{ij} (CO_2/N_2 and CO_2/CH_4) is defined as the ratio of downstream (y) mole fractions of two gases (y_i, y_j) to upstream (x) mole fractions of the same gases (x_i, x_j), given by Eq. 9:

$$\alpha_{ij} = \frac{y_i/y_j}{x_i/x_j} \quad (9)$$

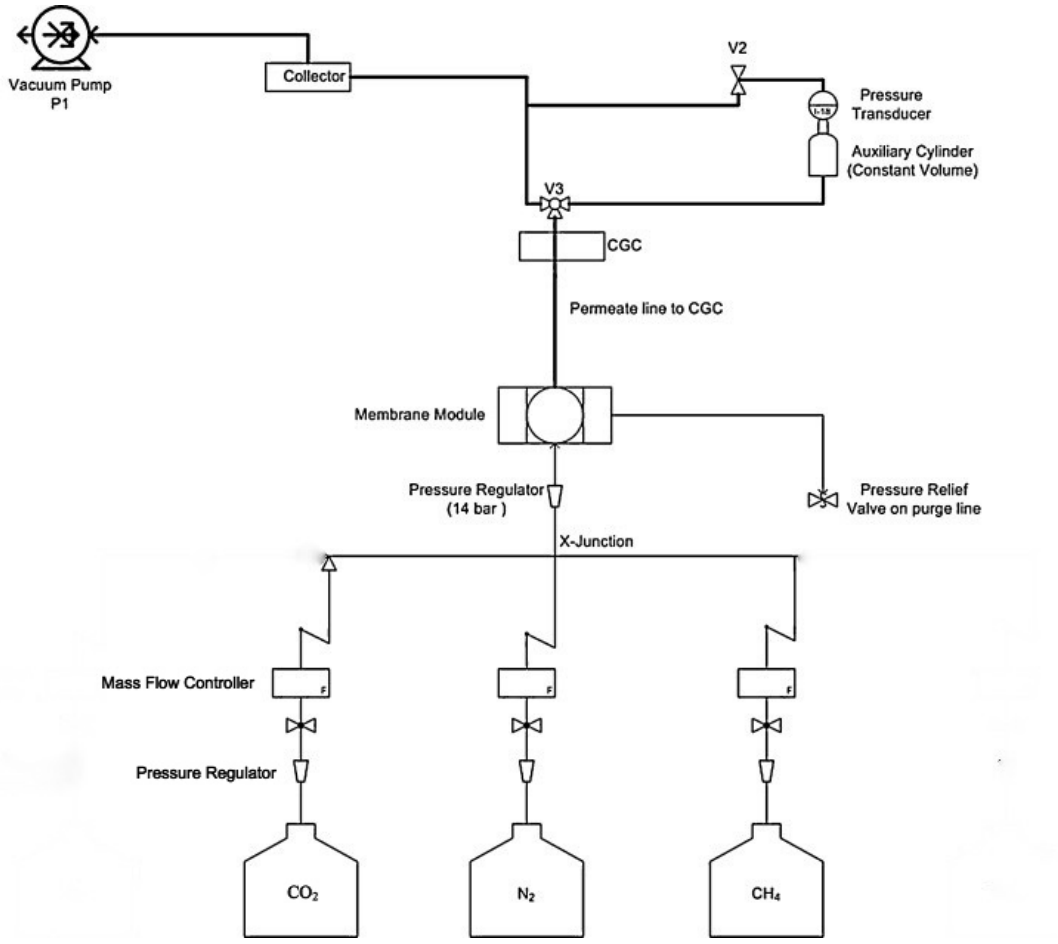

Figure 1: Gas permeation Setup

3. Results and Discussions

3.1. *Characterization of filler*

The XRD pattern of BIT-72 crystals is shown in Figure 2(a). The high intensity of the peaks (i.e. >2000 a.u.) signifies the highly crystalline nature of MOF particles. Sharp peaks also confirm the regular structure of the BIT-72 without any impurities. The characteristic peaks at θ = 6.9, 9.7, 11.8, 15.2, 17 and 18.2 are in exact agreement with the reported literature [42], and confirm the synthesis of pure BIT-72 crystals.

The FTIR spectrum of BIT-72 is exhibited in Figure 2(b). The broad peak from 3600 to 3100 cm^{-1} is attributed to a phenolic O-H stretch, while peaks of variable intensity around 2900 cm^{-1} correspond with carboxylic O-H and C-H stretches. The characteristic peaks of C-O stretch at 1246 cm^{-1}, C=O stretch at 1675 cm^{-1} and O-H bends at 1434.9 cm^{-1} further confirm the existence of

carboxylic acids. Peaks at 1589-740^{-1} (corresponding to a C=C stretch) and weak peaks at 2000-1650 cm^{-1} (C-H bending) are characteristic of an aromatic compound. These peaks confirm the presence of intact 2-hydroxy-1,4-benzenedicarboxylic acid linkers in BIT-72.

SEM images of formed BIT-72 nanoparticles at two different resolutions are presented in Figure 2(c). The images show regularly structured particles. Defined pebble-shaped MOF particles can be seen in the images. This also confirms the high crystallinity of the BIT-72 particles as reported in the XRD analysis. Most of the crystals are observed to be in size range of ~ 200 nm.

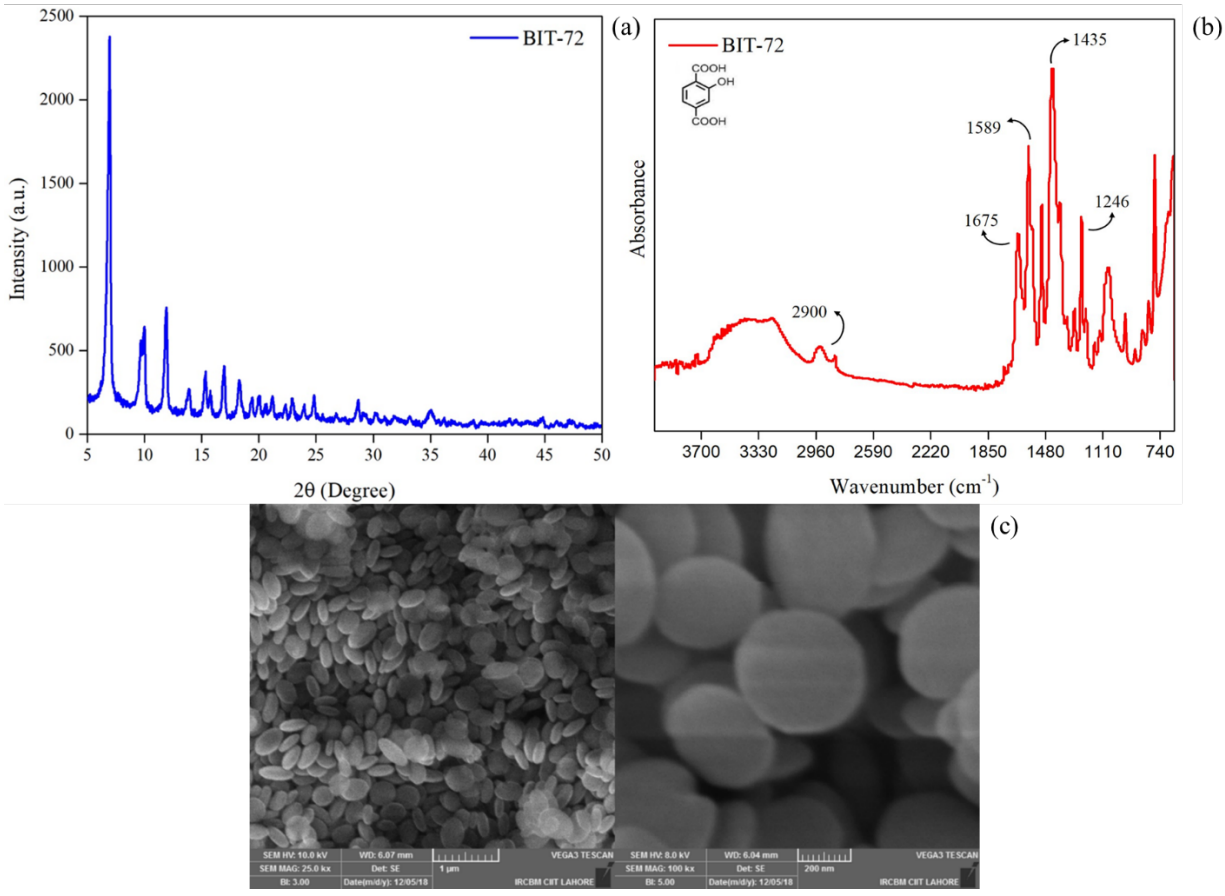

Figure 2: (a) XRD of BIT-72 (b) FTIR of BIT-72 (c) SEM images of BIT-72

3.2. Characterization of membrane

Cross-sectional SEM images of the membranes is illustrated in Figure 3. Compared to pure Pebax®1657 (Figure 3a), the addition of BIT-72 at different loading makes definite structural changes. On increasing the loading from 10% to 30 % (Figure 3b-d) the polymer becomes 'ragged' as a foreign entity is embedded into it and the membranes become rougher. The structure of BIT-

72 could be the reason for this phenomenon as it is uniformly dispersed across the membrane and its morphology could be unfavorably interacting with Pebax®1657. N_2 modified BIT-72 (Figure 6e) and O_2 modified BIT-72 (Figure 6f) have less effect of the MOF addition and the present smoother structures, similar to pure Pebax®1657 membranes but they are still different as seen in the images. This indicates that plasma modification yields groups on the BIT-72 surface that are more compatible with the polymer than those on the surface of the untreated parent structure.

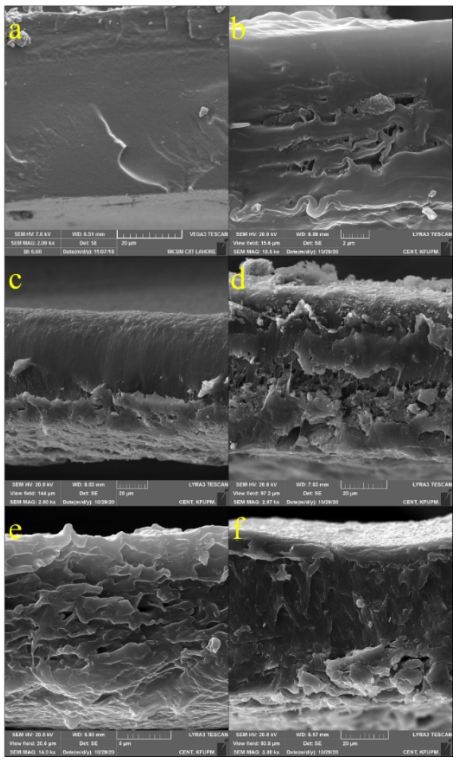

Figure 3: Cross-sectional SEM images of a) pure Pebax®1657, b) Pebax®1657/10 % BIT-72, c) Pebax®1657/20 % BIT-72, d) Pebax®1657/30 % BIT-72, e) Pebax®1657/30 % N_2-BIT-72 and f) Pebax®1657/30 % O_2-BIT-72

Fractional free volume (FFV) of a membrane is an important structural parameter that determines molecule transport channels and thus the gas diffusivity through the membrane. FFV depends upon the difference between experimental and theoretical values of membrane density, and is calculated by the buoyancy method that follows binary interaction principle [43]. Table 1 presents an increase in the values of density and FFV with increase in MOF loading. A rise in FFV leads to increase in diffusivity coefficient [44] and so in permeability. Pure Pebax®1657 membrane shows 1.21 g/cm^3 density which is gradually boosted to 1.32 g/cm^3 for 30% Pebax®1657 BIT-72 MMM with corresponding rise in FFV from 0.1 to 0.24. The free volume in pure Pebax®1657 membrane is the

gap between the polymer chains [45]. However, the inclusion of MOF creates more voids by its microcrystals and thus adds in the porosity of membrane. The slight increase in density may imply the formation of rigid structures around the MOF which favorably ensures good compatibility between the polymer and MOF [46]. It is interesting to note that plasma modification of 30% BIT-72 results in a decrease in density and FFV compared to the unmodified BIT-72. Density is reduced from 1.32 g/cm^3 to 1.26 g/cm^3 and 1.28 g/cm^3 for N_2 modified and O_2 modified 30% BIT-72 respectively. FFV also decreased from 0.24 to 0.15 and 0.18 for N_2 modified and O_2 modified 30% BIT-72 respectively. This indicates that the gas pathways are reduced in the plasma-modified BIT-72 prepared membranes.

Differential scanning calorimetry (DSC) analysis (Table 1) was used to reveal the chain packing and flexibility of the polymeric membranes on the basis of glass transition temperature (T_g) [47]. The T_g of pure Pebax®1657 was recorded at -53°C which agrees well with previous literature [48]. the T_g of the prepared MMMs gradually rises to -47.55 °C for 30% loading of BIT-72. The rise in T_g with the introduction of MOF indicates the enhanced rigidity and reduced flexibility of MMM which favors controlled permeability. Indeed, this variation in the thermal behavior of the MMMs presumes the formation of a dense structure around the MOF which is in accordance with the density and FTIR analysis (see above), and indicates that there are strong interactions between the polymer and MOF, even at higher loading [49].

Table 1: Density, Fractional Free Volume and Glass Transition Temperature (T_g) of prepared membranes

Membrane	Density g/cm^3	FFV (%)	T_g (°C)
Pure Pebax®1657	1.21	0.1	-53
Pebax®1657/10% BIT-72	1.24	0.13	-51
Pebax®165720% BIT-72	1.28	0.18	-48.4
Pebax®1657/30% BIT-72	1.32	0.24	-47.55
Pebax®1657/30% N_2-BIT-72	1.26	0.15	-49.54
Pebax®1657/30% O_2-BIT-72	1.28	0.18	-50.34

3.3. Membrane separation performance

The separation performances of the prepared MMMs were studied for both the single and mixed gas streams and the results were compared with those of the pure Pebax®1657 membrane. The permeability of pure gas was investigated for CO_2, CH_4 and N_2. The transport of gases through

dense MMMs is mainly governed by the solution-diffusion mechanism since the continuous phase is composed of polymer [42]. The incorporation of BIT-72 in Pebax®1657 enhances the permeability of each gas and improves the ideal selectivity of CO_2 over CH_4 and N_2, as is evident from Table 2. Compared with the pristine membrane, the MMM with 30% BIT-72 loading (30% Pebax®1657/BIT-72) increased the permeability of pure CO_2 by 70% and increased the ideal selectivities for CO_2/CH_4 and CO_2/N_2 to 43.5% and 16.7%, respectively. The permeability of a gas is determined by certain intrinsic properties, such as kinetic diameter, condensability, quadrupole moment, polarizability and its affinity towards a specific filler and polymer [50]. The kinetic diameter of a gas molecule is the principal factor for diffusivity such that there exists an inverse relationship between the two (i.e. diffusivity increases with decreasing kinetic diameter); therefore, the order of ease of diffusivity for the aforementioned gases with respect to their kinetic diameters is: CO_2 (0.33 nm) > N_2 (0.36 nm) > CH_4 (0.38 nm). Porous MOF allows the transference of molecules smaller than its pore size; however, if MOF pore opening is larger than incoming gas molecules then the microporosity of MOF assists the separation of smaller molecules from the bulkier ones [51]. The condensability of a gas is a function of its critical temperature and positively affects its solubility. The solubility order of the gases used in this work with respect to their condensability is: CO_2 (304.2 K) > CH_4 (191.5 K) > N_2 (126.2 K) [52]. The magnitude of the quadrupole moment of a molecule defines its capability of developing an attraction. The quadrupole moment of CO_2 (-13.4×10^{-40} C m^2) is significant, making it more likely to interact than N_2 (-4.72×10^{-40} C m^2). However, CH_4 is more polarizable than N_2 [53]. Hence, the intrinsic properties of gases imply that, of those used in this work, CO_2 molecules are supposed to be the most permeable which is in line with the results obtained. Other factors that influence the permeability of gases through MMMs involve the attributes of BIT-72, for example its high surface area, microporosity, affinity of is functional group (-OH) towards a gas as well as the structural and chemical characteristics of Pebax®1657 [54]. Since Pebax®1657 consists of 60% rubbery polyethyleneoxide (PEO) phase and 40% glassy polyamide (PA), the dipolar EO units dissolve polar gases and enhance the solubility of polarizable gases [48]. For pure Pebax®1657 membrane, the permeability of polar CO_2 is highest while that of CH_4 is greater than N_2, in line with their polarizabilities. The incorporation of BIT-72 into Pebax®1657 enhances the permeability of all gases because of its substantial surface area of 1413 m^2/g (as determined by BET analysis), inclusion of fractional free volume and increased porosity. The highest upswing in permeability of

CO_2 is also attributable to the pronounced affinity of hydroxyl groups (-OH) associated with BIT-72. When an electron-acceptor CO_2 molecule interacts with electron-donor –OH groups, an electron acceptor-donor complex is formed through hydrogen bonding [55]. The hydroxyl functional group induces a polar inner surface environment and increases the MOF's capacity for CO_2 uptake [31]. Despite being of a larger kinetic diameter, CH_4 showed a greater permeability than N_2 on account of its higher polarizability, better condensability and higher affinity towards the polymer and MOF. This demonstrate that MOFs do contribute in separation performance but ultimately polymer plays a governing role in overall results.

Table 2: Permeability and ideal selectivity of BIT-72 MMM

Membrane	Permeability (Barrer)			Selectivity	
	CO_2	CH_4	N_2	CO_2/CH_4	CO_2/N_2
Pure Pebax®1657	82	3.80	1.70	21.58	48.24
Pebax®1657/10% BIT-72	93	4.12	1.91	22.57	48.69
Pebax®165720% BIT-72	111	4.10	2.18	27.07	50.92
Pebax®1657/30% BIT-72	139	4.49	2.47	30.96	56.28

According to the results in Table 2, the increase in BIT-72 content in MMM improves the ideal selectivity of CO_2 over CH_4 and N_2, with the highest values achieved at a 30% loading. As mentioned before, CO_2 is more permeable than the other gases involved, thus further enhancement in permeability supports greater CO_2 permeation. The introduction of porosity, tortuosity and free volume are the main contributions of MOF to improving the separation performance of MMM. The CO_2/N_2 ideal selectivity results are superior to those of CO_2/CH_4 owing to lower sorption of N_2 than CH_4 through the membranes. The coefficients of diffusivity (D_i) and solubility (S_i) can provide more insight to the gas transport through membranes. Both coefficients exhibit a consistent and considerable rise upon increasing the loading of BIT-72, as shown in Figure 4. Diffusivity is led by three prime factors i.e. size of molecule, shape of molecule and FFV, thus, CO_2 molecules, being smaller in size (0.33 nm) and rod like in shape, can easily diffuse through MMMs with higher FFV. On the other hand, the CO_2-phillic nature of BIT-72 and Pebax®1657 justify the subsequent rise in its solubility.

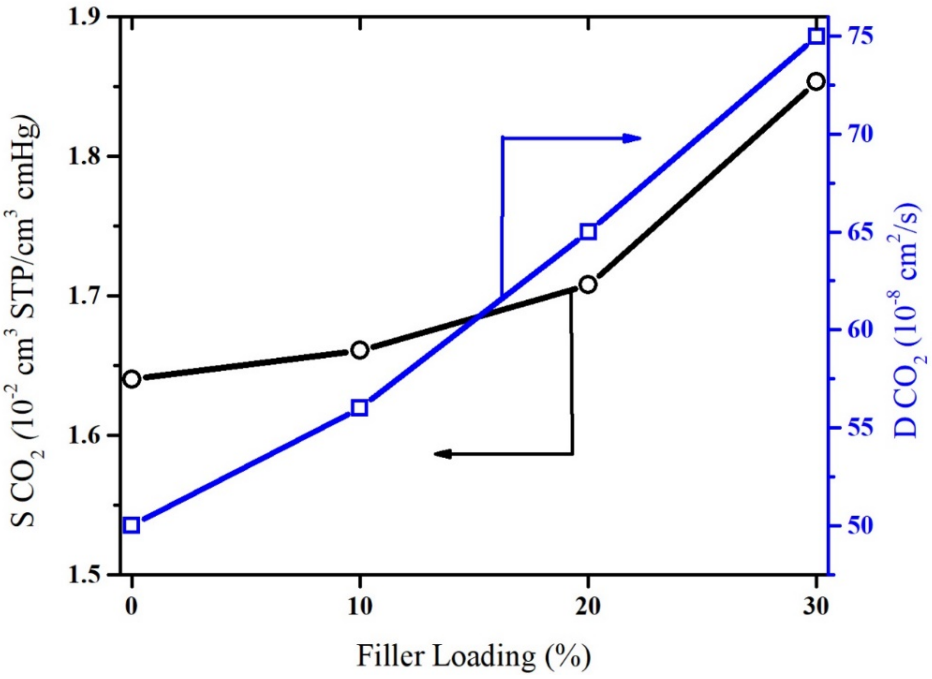

Figure 4: Effect of MOF loading on S_i and D_i of CO_2 in BIT-72 MMM

Mixed gas permeation analysis is essential as it provides a more accurate indication of the performance of the membranes in real industrial applications [56]. Experimental results illustrate same trends for the performance of the MMMs in mixed gas streams (50:50 binary mixtures) as the single gas stream (Table S1), although, there are consistent reductions in the corresponding permeability and selectivity results compared to those achieved with single gas streams for each wt% of MOF loading. The variation in the results for single and mixed gas tests can be ascribed to competitive sorption of penetrating gases, blocking effects of other types of molecules and gas phase non-ideality [3, 57].

The CO_2 permeability was studied as function of temperature by varying the temperature in range of 298K-338K while keeping the pressure constant at 10 bars (Figure S5). The results reveal that there exists a direct relationship between temperature and permeability which is attributed to an increase in fraction free volume following the "softening" of the polymer structure with an increase in temperature [58]. Since, BIT-72 is a rigid MOF, better permeation cannot be associated with the effect of temperature on MOF porosity. Thus, the only contribution temperature has in increasing the permeability lies in enhancing the diffusivity of gas molecules through the polymer matrix.

Activation energy (E_p) is defined as the minimum energy required by a penetrant molecule to surpass the "permeation barrier", hence the gases with lower E_p values more easily permeate. Increasing the temperature reduces the activation energy making CO_2 more permeable, the same result is achieved by incorporation of BIT-72 which minimizes the permeation barrier and facilitates the transport of gas molecules as given in Table 2.

Table 2: Activation energy of CO_2 in BIT-72 MMM

Membrane	Activation Energy of CO_2 E_p (kJ/mol)
Pure Pebax®1657	8.67
Pebax®1657/10% BIT-72	8.23
Pebax®165720% BIT-72	7.71
Pebax®1657/30% BIT-72	6.91

Since 30% loaded Pebax®1657/BIT-72 MMM showed the best results in terms of separation performance, these loadings were selected to carry out O_2 and N_2 plasma modification followed by fabrication of Pebax®1657/30% O_2-BIT-72 MMM and Pebax®1657/30% N_2-BIT-72 MMM to further investigate the separation efficiency. Plasma modified BIT-72 MMMs were tested for CO_2 recovery and performances were compared with unmodified MMM as presented in Table 3. N_2-Pebax®1657/BIT-72 and Pebax®1657/O_2-BIT-72MMMs showed enhanced CO_2 permeability and improved CO_2 selectivity over CH_4 and N_2, and N_2-modified BIT-72 produced the most promising results. It is believed that treatment of BIT-72 with O_2-plasma has produced more oxygen containing funtional groups (–OH, ─COOH) on the surface of MOF which contribute high electron density and hence resulted in increased affinity for the CO_2 quadrapole [59, 60]. Since the N_2-plasma treatment of BIT-72 might have introduced nitrogen containing funtional groups i.e $–NH_3$, $─NH_{2j,}$ which possess even higher affinities for CO_2 due to their capability of producing electron donor-acceptor complexes with CO_2 and, therefore, showed improved CO_2 permeability [61]. There exists the possibility of N-H-O hydrogen bonding and interactions between the N lone pair and the carbon of CO_2 [62]. Moreover, $-NH_2$ may also boosts the intrinsic acidity of bridging –OH groups, thereby increasing CO_2-OH interactivity [50]. CO_2 selectivity over CH_4 and N_2 is improved by 20.41% and 17.6%, respectively, for Pebax®1657/O_2-BIT-72 MMM and 39% and

29%, respectively, for Pebax®1657/N_2-BIT-72. Conclusively, Plasma treatment induces polarity on MOF surface, though, excessive exposure to plasma may alter the MOF structure. The comparison of the D_i and S_i of modified and unmodified MMMs can provide a better perception of transport phenomena.

Table 3: Permeability and ideal selectivity of plasma treated BIT-72 MMM

Membrane	Permeability (Barrer)			Selectivity	
	CO_2	CH_4	N_2	CO_2/CH_4	CO_2/N_2
Pebax®1657/30% BIT-72	139	4.49	2.47	30.96	56.28
Pebax®1657/30% N_2-BIT-72	146	3.39	2.01	43.07	72.64
Pebax®1657/30% O_2-BIT-72	145	3.89	2.19	37.28	66.21

It is evident from Figure 5, S_i has increased for modified MMMs owing to the higher CO_2 affinities of introduced –OH and -NH_3 groups in plasma treated MOF. The trend of D_i is, however, the opposite. The decreasing trend for modified MMMs is the consequence of increased tortuosity caused by the inclusion of bulky –OH and –NH_3 groups [50]. The lowest diffusivity coefficient for N_2-plasma modified MMM might also be ascribable possible interactions of CO2 with modified BIT-72 [61]. Moreover, amine groups are bulkier and obstruct the pore channels making them narrow. The overall increase in CO_2 permeability in modified MMM is, therefore, assigned to increased sorption. These results are also supported by FFV values which indicated decrease in gas pathways by having low FFV values.

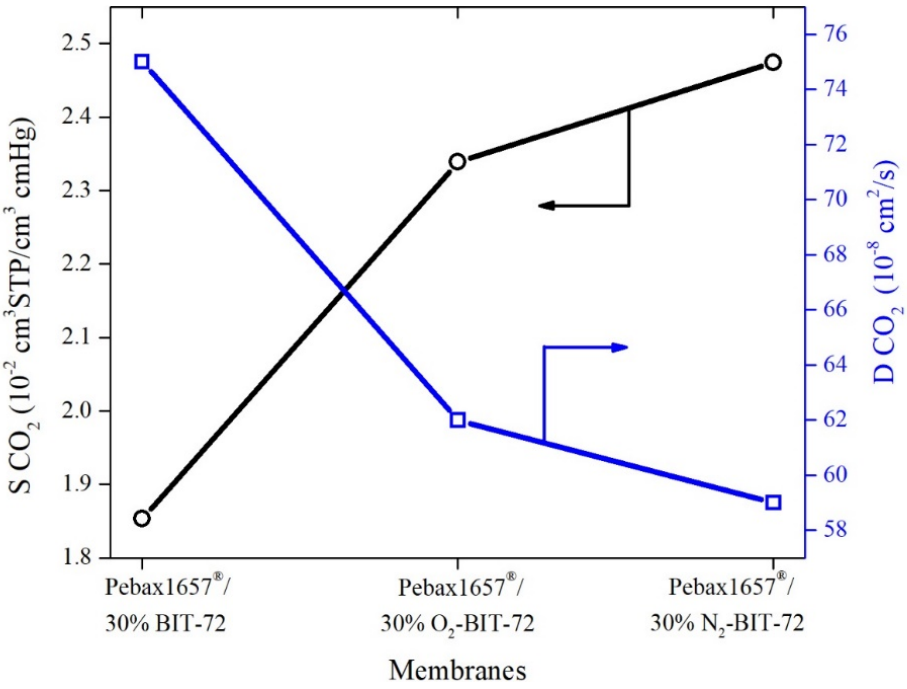

Figure 5: S_i and D_i of plasma treated BIT-72 MMM

Mixed gas results of plasma modified BIT-72 MMMs compared with 30% BIT-72 MMM are presented in Table S2. The results demonstrate classic lowering of permeability and selectivity of gasses for mixed gasses for plasma modified BIT-72 membranes. Overall, the permeation trend is similar to pure gas permeabilities. The mixed gas selectivity is decreased by 5% for CO_2/CH_4 and by for 3% CO_2/N_2 in 30% N_2-BIT-72 membrane. In membrane of O_2-BIT-72 selectivity decreased for CO_2/CH_4 is 2% and for CO_2/N_2 is 1%. Noticeably, the decrease in mixed gas selectivity for 30% BIT-72 (6% for CO_2/CH_4 and by for 5% CO_2/N_2) is greater than plasma modified BIT-72 MMMs. This demonstrates the effectiveness of plasma modification of 30% BIT-72.

The temperature dependency of permeability was also investigated for plasma modified BIT-72 MMMs and is illustrated in Figure S6. The temperature range used was same as that used for unmodified BIT-72 MMMs. Here again, permeability was increased with the rise in temperature demonstrating a direct correlation. 30% N_2-BIT-72 MMM and 30% O_2-BIT-72 MMM had similar increases in permeability with similar values. The permeabilities values were greater for plasma modified BIT-72 MMMs as compared to 30% BIT-72 MMM.

E_p of the 30% N_2-BIT-72 and 30% O_2-BIT-72 MMMs along with 30% BIT-72 is presented in Table 4. 30% BIT-72 demonstrated the lowest E_p of all the membranes and increased permeability

of plasma modified BIT-72 MMMs is supported by E_p values of plasma modified BIT-72 MMMs. The results demonstrate ease of permeability in plasma modified BIT-72 MMMs. These results are consistent with all of the results stated above.

Table 4: Activation energy of CO_2 in plasma treated BIT-72 MMM

Membrane	Activation Energy of CO_2 E_p (kJ/mol)
Pebax®1657/30% BIT-72	6.9
Pebax®1657/30% N_2-BIT-72	6.5
Pebax®1657/30% O_2-BIT-72	6.3

4. Comparison with state-of-the-art membranes

Before comparing the prepared membranes with other membranes in literature, it is essential to compare the prepared membranes with each other. BIT-72 MMMs showed increasing trend of CO_2 permeability and CO_2/CH_4 / CO_2/N_2 selectivity with increased loading (Table S3). All the BIT-72 MMM had greater CO_2 permeability and CO_2/CH_4 / CO_2/N_2 selectivity as compared to pure Pebax®1657 membranes. Plasma modified BIT-72 MMMs had even greater increase in CO_2 permeability and CO_2/CH_4 / CO_2/N_2 selectivity. CO_2 permeability was increased by 5% and 4% for 30% N_2-BIT-72 and 30% O_2-BIT-72 respectively. In 30% N_2-BIT-72 MMM CO_2/CH_4 selectivity had a staggering increase of 39% followed by 29% increase in CO_2/N_2 selectivity. In 30% O_2-BIT-72 MMM the increase in CO_2/CH_4 selectivity was 20% and for CO_2/N_2 selectivity was 18%. The accretion in CO_2 permeability was not substantial because plasma modification reduced the FFV and densities values. The overall increase in CO_2 permeability was attributed to S_i because of the addition of CO_2-philic groups to plasma modified BIT-72. Mixed gas permeability of plasma modified BIT-72 MMMs (137 Barrer for 30% N_2-BIT-72 and 141 Barrer for 30% O_2-BIT-72) was in the range of ideal gas CO_2 permeability (139 Barrer). This demonstrates that plasma modified BIT-72 MMM are indeed a promising route for membrane fabrication as the mixed gas permeability is the range of ideal gas permeability and consequently ideal gas permeability would be far greater.

The results of recent studies wherein different fillers have been incorporated in Pebax®1657 are reported in Table S3. There exists a vast variety of work that has been done with Pebax®1657 based MMMs. Fan *et.al* incorporated two MOFs (Ni2(L-asp)2bipy and Ni2(L-asp)2pz) with tunable pore sizes into a copolymer (poly-ether-block-amide (Pebax®1657)) and achieved an increased CO_2 permeability (P_{CO2}) of 120.2 Barrers; however, the CO_2/CH_4 selectivity ($S_{CO2/CH4}$) was below 30 [3]. Meshkat *et.al* studied CO_2 separation by embedding Pebax®1657 with amine modified- MIL-53(Al) to analyze the impact of functionalization of MOF and the results attained were very positive with a 174% increase in CO_2 permeability compared to the neat Pebax®1657 membrane [50]. Sutrisna *et al* and ahmed *et al* overcame challenges like interfacial compatibility and plasticization through surface modification and functionalization of UiO-66 and achieved extraordinary separation performances [63]. Different membrane configurations of MMMs with the same filler and polymer i.e ZIF-8 and Pebax®1657 respectively, had different impacts on the membrane performances for CO_2 separation [64]. Dorosti *et.al* fabricated FeBTC based MMMs using the same polymer and obtained an optimal CO_2 permeability of 329.7 Barrer with $S_{CO2/CH4}$ of 20.9 for 30% loading [65]. The effect of MOF functionalization upon its interaction with a polymer matrix is studied by Khosravi *et.al*, who reported an increase in membrane selectivity because of the hydrogen bonding which developed between NH_2-CuBTC and Pebax®1657 [66]. Pebax®1657 has been incorporated with numerous fillers including ZIF-7, Zeolite 4A, PEG-POSS, MWCNTs, SAPO-34 etc, and exhibited satisfactory performances with respect to CO_2 removal. However, the membranes fabricated in this work with BIT-72 impregnated in Pebax®1657 have excelled in separation performance with 139 Barrer CO_2 permeability with appreciable selectivities of 30.96 and 56.28 for CO_2/CH_4 and CO_2/N_2, respectively.

Figure 6 illustrates the results of this study plotted on a Robeson upper bound plot for better comparison of parameter performances with other well-known works. Pure Pebax®1657 itself lies very close to the upper bound, showcasing its superior properties, showing high permeability but relatively low selectivity. BIT-72 MMMs not only enhance the permeability but there is a significant increase in selectivity. For CO_2/CH_4, 30% BIT-72 loading membrane lies exactly on the upper bound. For CO_2/N_2 30% BIT-72 loading membrane it is just below the upper bound. This demonstrates that the membranes prepared in this work showcased superior performances. In case of O_2 and N_2 plasma-modified BIT-72 membranes, the Robeson's upper bound is crossed for CO_2/CH_4 gas mixtures. For CO_2/N_2 gas mixtures, the O_2 modified BIT-72 is almost touching the

upper bound and the N_2 modified BIT-72 falls on the upper bound. Overall, plasma modification of BIT-72 produced impressive results.

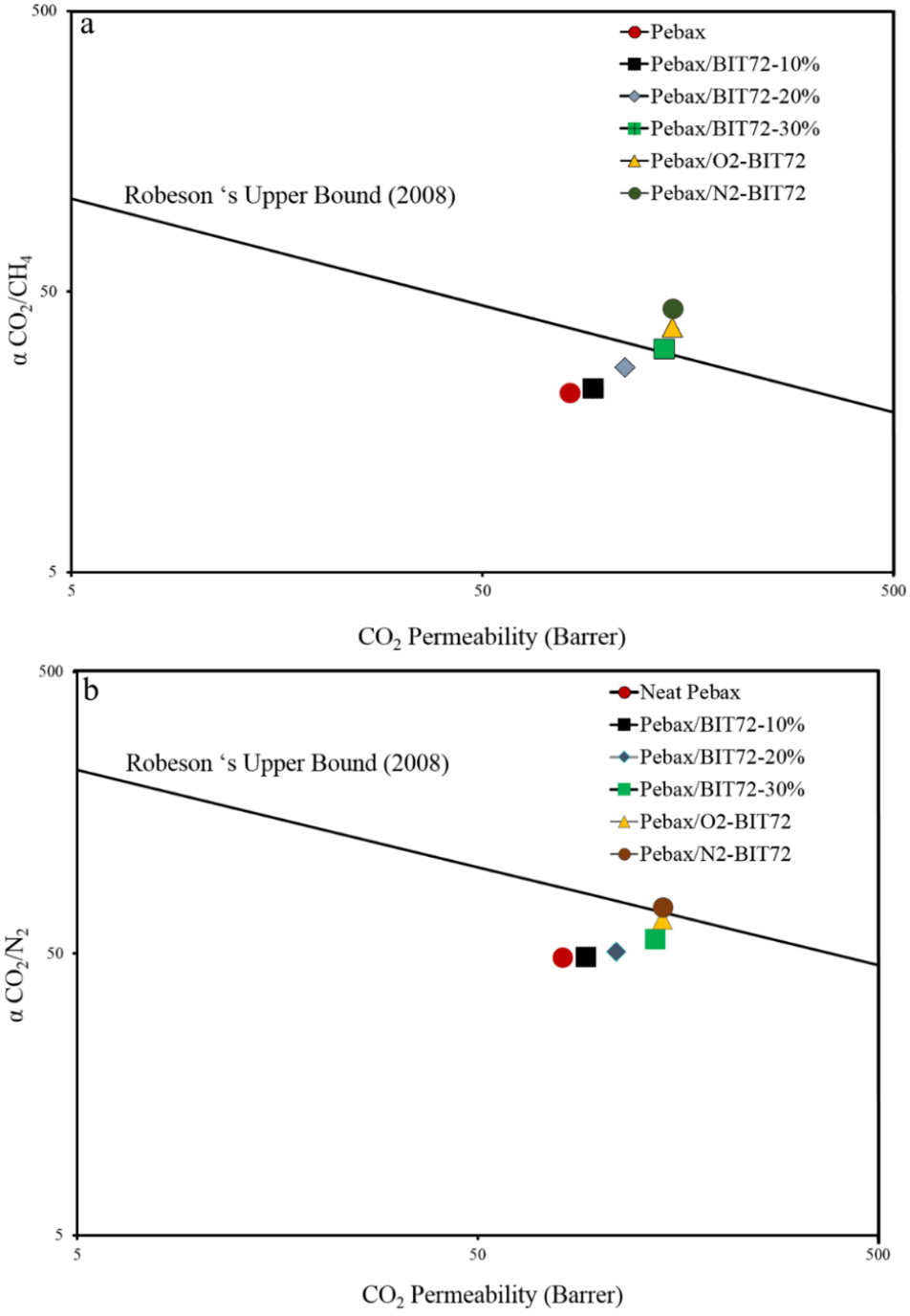

Figure 6: Robeson upper bound plot for a) CO_2/CH_4 and b) CO_2/N_2

5. Conclusion

In summary, MMMs containing BIT-72 filler and Pebax®1657 polymer were successfully fabricated. The comparison of MMMs with different loadings of BIT-72 and pure Pebax®1657 membrane was studied. The high crystallinity of MOF was confirmed by SEM and XRD analysis while greater surface area was assured by BET test. Increasing the BIT-72 loading in membranes enhanced CO_2 permeability and selectivity over CH_4 and N_2. The CO_2/CH_4 selectivity was increased by 43.5% and CO_2/N_2 selectivity was increased by 16.7% with enhanced CO_2 permeability of 139 Barrer at 30% filler loading. Diffusion solubility played an integral role in the increase of permeability of CO_2 which resulted in a higher selectivity. Plasma modification of BIT-72 yielded encouraging results as both permeability and selectivity was increased for CO_2/CH_4 and CO_2/N_2 gas mixtures. There was an increase of 20.7% and 17.6% for CO_2/CH_4 and CO_2/CH_4, respectively, for O_2 modified BIT-72. For N_2 modified BIT-72 these results were even better, showing an increase of 39.5% and 28.9% for CO_2/CH_4 and CO_2/CH_4, respectively. Surprisingly, the solubility coefficient played a leading role in the elevation of permeability and selectivity. This study presented exceptional gas separation performance. Understanding the chemistry and morphological changes of plasma modified MOF can lead to preparation of improved and sophisticated membranes with superior performance.

Acknowledgements

The authors would like to acknowledge the support provided by the Deanship of Research (DSR) at King Fahd University of Petroleum and Minerals (KFUPM) for funding this work through project No. DF181004.

References

[1] C. Song, "Global challenges and strategies for control, conversion and utilization of CO2 for sustainable development involving energy, catalysis, adsorption and chemical processing," *Catalysis today,* vol. 115, pp. 2-32, 2006.

[2] M. H. Al-Marzouqi, S. A. Marzouk, M. H. El-Naas, and N. Abdullatif, "CO2 removal from CO2− CH4 gas mixture using different solvents and hollow fiber membranes," *Industrial & engineering chemistry research,* vol. 48, pp. 3600-3605, 2009.

[3] L. Fan, Z. Kang, Y. Shen, S. Wang, H. Zhao, H. Sun*, et al.*, "Mixed Matrix Membranes Based on Metal–Organic Frameworks with Tunable Pore Size for CO2 Separation," *Crystal Growth & Design,* vol. 18, pp. 4365-4371, 2018.

[4] H. Huang, Y. Shi, W. Li, and S. Chang, "Dual alkali approaches for the capture and separation of CO2," *Energy & fuels,* vol. 15, pp. 263-268, 2001.
[5] M. T. Ho, G. W. Allinson, and D. E. Wiley, "Reducing the cost of CO2 capture from flue gases using pressure swing adsorption," *Industrial & Engineering Chemistry Research,* vol. 47, pp. 4883-4890, 2008.
[6] F. Zheng, D. N. Tran, B. J. Busche, G. E. Fryxell, R. S. Addleman, T. S. Zemanian*, et al.*, "Ethylenediamine-modified SBA-15 as regenerable CO2 sorbent," *Industrial & engineering chemistry research,* vol. 44, pp. 3099-3105, 2005.
[7] A. A. Olajire, "CO2 capture and separation technologies for end-of-pipe applications–a review," *Energy,* vol. 35, pp. 2610-2628, 2010.
[8] H. Yang, Z. Xu, M. Fan, R. Gupta, R. B. Slimane, A. E. Bland*, et al.*, "Progress in carbon dioxide separation and capture: A review," *Journal of environmental sciences,* vol. 20, pp. 14-27, 2008.
[9] W. Han, C. Zhang, M. Zhao, F. Yang, Y. Yang, and Y. Weng, "Post-modification of PIM-1 and simultaneously in situ synthesis of porous polymer networks into PIM-1 matrix to enhance CO2 separation performance," *Journal of Membrane Science,* vol. 636, p. 119544, 2021.
[10] F. Li, C. Zhang, and Y. Weng, "Preparation and Gas Separation Properties of Triptycene-Based Microporous Polyimide," *Macromolecular Chemistry and Physics,* vol. 220, p. 1900047, 2019.
[11] J. Wu, S. Japip, and T.-S. Chung, "Infiltrating molecular gatekeepers with coexisting molecular solubility and 3D-intrinsic porosity into a microporous polymer scaffold for gas separation," *Journal of Materials Chemistry A,* vol. 8, pp. 6196-6209, 2020.
[12] F. A. Rahman, M. M. A. Aziz, R. Saidur, W. A. W. A. Bakar, M. Hainin, R. Putrajaya*, et al.*, "Pollution to solution: Capture and sequestration of carbon dioxide (CO2) and its utilization as a renewable energy source for a sustainable future," *Renewable and Sustainable Energy Reviews,* vol. 71, pp. 112-126, 2017.
[13] J. Pires, F. Martins, M. Alvim-Ferraz, and M. Simões, "Recent developments on carbon capture and storage: an overview," *Chemical engineering research and design,* vol. 89, pp. 1446-1460, 2011.
[14] P. Gauvillé, J.-C. Foucher, and D. Moreau, "Achievable combustion efficiency with Alstom CFB boilers for burning discarded coal," *Journal of the Southern African Institute of Mining and Metallurgy,* vol. 112, pp. 437-447, 2012.
[15] A. L. Khan, N. Habib, and M. Aslam, "Metal organic frameworks-based mixed matrix membranes for gas separation," in *Nanomaterials for Air Remediation*, ed: Elsevier, 2020, pp. 273-292.
[16] Z. Shamair, N. Habib, M. A. Gilani, and A. L. Khan, "Theoretical and experimental investigation of CO2 separation from CH4 and N2 through supported ionic liquid membranes," *Applied Energy,* vol. 268, p. 115016, 2020.
[17] M. Aroon, A. Ismail, T. Matsuura, and M. Montazer-Rahmati, "Performance studies of mixed matrix membranes for gas separation: a review," *Separation and purification Technology,* vol. 75, pp. 229-242, 2010.
[18] H. Cong, M. Radosz, B. F. Towler, and Y. Shen, "Polymer–inorganic nanocomposite membranes for gas separation," *Separation and purification technology,* vol. 55, pp. 281-291, 2007.

[19] O. Yaghi and H. Li, "Hydrothermal synthesis of a metal-organic framework containing large rectangular channels," *Journal of the American Chemical Society,* vol. 117, pp. 10401-10402, 1995.
[20] M. Usman, M. Ali, B. A. Al-Maythalony, A. S. Ghanem, O. W. Saadi, M. Ali*, et al.*, "Highly Efficient Permeation and Separation of Gases with Metal–Organic Frameworks Confined in Polymeric Nanochannels," *ACS Applied Materials & Interfaces,* vol. 12, pp. 49992-50001, 2020.
[21] J. Deng, Z. Dai, J. Hou, and L. Deng, "Morphologically tunable MOF nanosheets in mixed matrix membranes for CO2 separation," *Chemistry of Materials,* vol. 32, pp. 4174-4184, 2020.
[22] N. Habib, Z. Shamair, N. Tara, A.-S. Nizami, F. H. Akhtar, N. M. Ahmad*, et al.*, "Development of highly permeable and selective mixed matrix membranes based on Pebax® 1657 and NOTT-300 for CO2 capture," *Separation and Purification Technology,* vol. 234, p. 116101, 2020.
[23] I. Yasmeen, A. Ilyas, Z. Shamair, M. A. Gilani, S. Rafiq, M. R. Bilad*, et al.*, "Synergistic effects of highly selective ionic liquid confined in nanocages: Exploiting the three component mixed matrix membranes for CO2 Capture," *Chemical Engineering Research and Design,* 2020.
[24] C. Y. Chuah, J. Lee, J. Song, and T.-H. Bae, "CO2/N2 separation properties of polyimide-based mixed-matrix membranes comprising UiO-66 with various functionalities," *Membranes,* vol. 10, p. 154, 2020.
[25] T. Xu, J. Yang, J. Liu, and Q. Fu, "Surface modification of multi-walled carbon nanotubes by O2 plasma," *Applied Surface Science,* vol. 253, pp. 8945-8951, 2007.
[26] M. Mollah, R. Schennach, J. Patscheider, S. Promreuk, and D. L. Cocke, "Plasma chemistry as a tool for green chemistry, environmental analysis and waste management," *Journal of hazardous materials,* vol. 79, pp. 301-320, 2000.
[27] M. Mozetič, A. Zalar, P. Panjan, M. Bele, S. Pejovnik, and R. Grmek, "A method of studying carbon particle distribution in paint films," *Thin Solid Films,* vol. 376, pp. 5-8, 2000.
[28] L. Shao, J. Samseth, and M. B. Hägg, "Effect of Plasma Treatment on the Gas Permeability of Poly (4-methyl-2-pentyne) Membranes," *Plasma Processes and Polymers,* vol. 4, pp. 823-831, 2007.
[29] J. B. Decoste, G. W. Peterson, M. W. Smith, C. A. Stone, and C. R. Willis, "Enhanced stability of Cu-BTC MOF via perfluorohexane plasma-enhanced chemical vapor deposition," *Journal of the American Chemical Society,* vol. 134, pp. 1486-1489, 2012.
[30] S.-J. Park and J.-S. Kim, "Influence of plasma treatment on microstructures and acid–base surface energetics of nanostructured carbon blacks: N2 plasma environment," *Journal of colloid and interface science,* vol. 244, pp. 336-341, 2001.
[31] H. Li, X. Feng, D. Ma, M. Zhang, Y. Zhang, Y. Liu*, et al.*, "Stable aluminum metal–organic frameworks (Al-MOFs) for balanced CO2 and water selectivity," *ACS applied materials & interfaces,* vol. 10, pp. 3160-3163, 2018.
[32] P. M. Schoenecker, C. G. Carson, H. Jasuja, C. J. Flemming, and K. S. Walton, "Effect of water adsorption on retention of structure and surface area of metal–organic frameworks," *Industrial & Engineering Chemistry Research,* vol. 51, pp. 6513-6519, 2012.
[33] P. D. Sutrisna, J. Hou, H. Li, Y. Zhang, and V. Chen, "Improved operational stability of Pebax-based gas separation membranes with ZIF-8: A comparative study of flat sheet and

composite hollow fibre membranes," *Journal of membrane science,* vol. 524, pp. 266-279, 2017.
[34] B. Yu, H. Cong, Z. Li, J. Tang, and X. S. Zhao, "Pebax-1657 nanocomposite membranes incorporated with nanoparticles/colloids/carbon nanotubes for CO2/N2 and CO2/H2 separation," *Journal of Applied Polymer Science,* vol. 130, pp. 2867-2876, 2013.
[35] S. Habibzare, M. Asghari, and A. Djirsarai, "Nano composite PEBAX®/PEG membranes: Effect of MWNT filler on CO2/CH4 separation," *International Journal of Nano Dimension,* vol. 5, pp. 247-254, 2014.
[36] M. Isanejad, N. Azizi, and T. Mohammadi, "Pebax membrane for CO2/CH4 separation: Effects of various solvents on morphology and performance," *Journal of Applied Polymer Science,* vol. 134, 2017.
[37] X. Tu and J. Whitehead, "Plasma-catalytic dry reforming of methane in an atmospheric dielectric barrier discharge: Understanding the synergistic effect at low temperature," *Applied Catalysis B: Environmental,* vol. 125, pp. 439-448, 2012.
[38] B. D. Freeman, "Basis of permeability/selectivity tradeoff relations in polymeric gas separation membranes," *Macromolecules,* vol. 32, pp. 375-380, 1999.
[39] A. L. Khan, S. Basu, A. Cano-Odena, and I. F. Vankelecom, "Novel high throughput equipment for membrane-based gas separations," *Journal of membrane science,* vol. 354, pp. 32-39, 2010.
[40] M. Li, X. Zhang, S. Zeng, H. Gao, J. Deng, Q. Yang*, et al.*, "Pebax-based composite membranes with high gas transport properties enhanced by ionic liquids for CO 2 separation," *RSC advances,* vol. 7, pp. 6422-6431, 2017.
[41] H. L. Frisch, "The time lag in diffusion," *The Journal of Physical Chemistry,* vol. 61, pp. 93-95, 1957.
[42] N. N. Li, A. G. Fane, W. W. Ho, and T. Matsuura, *Advanced membrane technology and applications*: John Wiley & Sons, 2011.
[43] Y. Li, Q. Xin, H. Wu, R. Guo, Z. Tian, Y. Liu*, et al.*, "Efficient CO 2 capture by humidified polymer electrolyte membranes with tunable water state," *Energy & Environmental Science,* vol. 7, pp. 1489-1499, 2014.
[44] M. H. Cohen and D. Turnbull, "Molecular transport in liquids and glasses," *The Journal of Chemical Physics,* vol. 31, pp. 1164-1169, 1959.
[45] X. Wu, Z. Tian, S. Wang, D. Peng, L. Yang, Y. Wu*, et al.*, "Mixed matrix membranes comprising polymers of intrinsic microporosity and covalent organic framework for gas separation," *Journal of Membrane Science,* vol. 528, pp. 273-283, 2017.
[46] S. Shahid and K. Nijmeijer, "High pressure gas separation performance of mixed-matrix polymer membranes containing mesoporous Fe (BTC)," *Journal of membrane science,* vol. 459, pp. 33-44, 2014.
[47] J. Yuan, H. Zhu, J. Sun, Y. Mao, G. Liu, and W. Jin, "Novel ZIF-300 mixed-matrix membranes for efficient CO2 capture," *ACS applied materials & interfaces,* vol. 9, pp. 38575-38583, 2017.
[48] A. Car, C. Stropnik, W. Yave, and K.-V. Peinemann, "PEG modified poly (amide-b-ethylene oxide) membranes for CO2 separation," *Journal of Membrane Science,* vol. 307, pp. 88-95, 2008.
[49] Z. K. Zhu, Y. Yang, J. Yin, and Z. N. Qi, "Preparation and properties of organosoluble polyimide/silica hybrid materials by sol–gel process," *Journal of Applied Polymer Science,* vol. 73, pp. 2977-2984, 1999.

[50] S. Meshkat, S. Kaliaguine, and D. Rodrigue, "Mixed matrix membranes based on amine and non-amine MIL-53 (Al) in Pebax® MH-1657 for CO2 separation," *Separation and Purification Technology,* vol. 200, pp. 177-190, 2018.
[51] M. Valero, B. Zornoza, C. Téllez, and J. Coronas, "Mixed matrix membranes for gas separation by combination of silica MCM-41 and MOF NH2-MIL-53 (Al) in glassy polymers," *Microporous and mesoporous materials,* vol. 192, pp. 23-28, 2014.
[52] B. E. Poling, J. M. Prausnitz, and J. P. O'connell, *The properties of gases and liquids* vol. 5: Mcgraw-hill New York, 2001.
[53] R. S. Murali, A. Ismail, M. Rahman, and S. Sridhar, "Mixed matrix membranes of Pebax-1657 loaded with 4A zeolite for gaseous separations," *Separation and Purification Technology,* vol. 129, pp. 1-8, 2014.
[54] L. Dong, M. Chen, J. Li, D. Shi, W. Dong, X. Li*, et al.*, "Metal-organic framework-graphene oxide composites: A facile method to highly improve the CO2 separation performance of mixed matrix membranes," *Journal of membrane science,* vol. 520, pp. 801-811, 2016.
[55] A. Vimont, A. Travert, P. Bazin, J.-C. Lavalley, M. Daturi, C. Serre*, et al.*, "Evidence of CO 2 molecule acting as an electron acceptor on a nanoporous metal–organic-framework MIL-53 or Cr 3+(OH)(O 2 C–C 6 H 4–CO 2)," *Chemical Communications,* pp. 3291-3293, 2007.
[56] R. W. Baker and B. T. Low, "Gas separation membrane materials: a perspective," *Macromolecules,* vol. 47, pp. 6999-7013, 2014.
[57] P. Tin, T. Chung, Y. Liu, R. Wang, S. Liu, and K. Pramoda, "Effects of cross-linking modification on gas separation performance of Matrimid membranes," *Journal of Membrane Science,* vol. 225, pp. 77-90, 2003.
[58] L. Liu, A. Chakma, and X. Feng, "CO2/N2 separation by poly (ether block amide) thin film hollow fiber composite membranes," *Industrial & engineering chemistry research,* vol. 44, pp. 6874-6882, 2005.
[59] T. Trantidou, Y. Elani, E. Parsons, and O. Ces, "Hydrophilic surface modification of PDMS for droplet microfluidics using a simple, quick, and robust method via PVA deposition," *Microsystems & nanoengineering,* vol. 3, pp. 1-9, 2017.
[60] C. Tenney and C. Lastoskie, "Molecular simulation of carbon dioxide adsorption in chemically and structurally heterogeneous porous carbons," *Environmental Progress,* vol. 25, pp. 343-354, 2006.
[61] F. de Clippel, A. L. Khan, A. Cano-Odena, M. Dusselier, K. Vanherck, L. Peng*, et al.*, "CO 2 reverse selective mixed matrix membranes for H 2 purification by incorporation of carbon–silica fillers," *Journal of Materials Chemistry A,* vol. 1, pp. 945-953, 2013.
[62] R. Vaidhyanathan, S. S. Iremonger, G. K. Shimizu, P. G. Boyd, S. Alavi, and T. K. Woo, "Direct observation and quantification of CO2 binding within an amine-functionalized nanoporous solid," *Science,* vol. 330, pp. 650-653, 2010.
[63] M. Z. Ahmad, M. Navarro, M. Lhotka, B. Zornoza, C. Téllez, W. M. de Vos*, et al.*, "Enhanced gas separation performance of 6FDA-DAM based mixed matrix membranes by incorporating MOF UiO-66 and its derivatives," *Journal of membrane science,* vol. 558, pp. 64-77, 2018.
[64] A. Jomekian, R. M. Behbahani, T. Mohammadi, and A. Kargari, "High speed spin coating in fabrication of Pebax 1657 based mixed matrix membrane filled with ultra-porous ZIF-8

particles for CO 2/CH 4 separation," *Korean Journal of Chemical Engineering,* vol. 34, pp. 440-453, 2017.

[65] F. Dorosti and A. Alizadehdakhel, "Fabrication and investigation of PEBAX/Fe-BTC, a high permeable and CO2 selective mixed matrix membrane," *Chemical Engineering Research and Design,* vol. 136, pp. 119-128, 2018.

[66] T. Khosravi, M. Omidkhah, S. Kaliaguine, and D. Rodrigue, "Amine-functionalized CuBTC/poly (ether-b-amide-6)(Pebax® MH 1657) mixed matrix membranes for CO2/CH4 separation," *The Canadian Journal of Chemical Engineering,* vol. 95, pp. 2024-2033, 2017.